ELSEVIER

Journal of Alloys and Compounds 455 (2008) 203–206

Journal of ALLOYS AND COMPOUNDS

www.elsevier.com/locate/jallcom

Magnetostriction and corrosion resistance of $Tb_{0.3}Dy_{0.7}(Fe_{1-x}Si_x)_{1.95}$ alloys

Lihong Xu, Chengbao Jiang *, Chungen Zhou, Huibin Xu

Department of Materials Science and Engineering, Beijing University of Aeronautics and Astronautics, Beijing 100083, PR China

Received 17 November 2006; received in revised form 13 January 2007; accepted 15 January 2007
Available online 19 January 2007

Abstract

Magnetostriction and corrosion resistance in 3.5% NaCl solution of as-cast $Tb_{0.3}Dy_{0.7}(Fe_{1-x}Si_x)_{1.95}$ ($x = 0$, 0.025 and 0.10) alloys were studied. With little Si addition, $Tb_{0.3}Dy_{0.7}(Fe_{0.975}Si_{0.025})_{1.95}$ alloy possesses both giant magnetostriction and improved corrosion resistance. The reason for improved corrosion resistance is suggested to be the increased natural corrosion potential E_{corr} for the rare earth-rich phase and the reduced electrochemical potential difference between the rare earth-rich phase and the matrix phase in TbDyFeSi alloys.

Keywords: Magnetostriction; Corrosion; Si addition; TbDyFe alloy

1. Introduction

Cubic Laves phase compound $Tb_{0.3}Dy_{0.7}Fe_{1.95}$ alloy (abbreviated as TbDyFe) exhibiting giant magnetostriction attracts considerable attention in the last decades [1,2]. The material has shown many potential applications especially in sonar equipment and petroleum production. Considerable efforts have been taken to investigate the element addition effect in $Tb_{0.3}Dy_{0.7}(Fe_{1-x}T_x)_{1-y}$ (T = Al, Co, Be and B) (abbreviated as TbDyFeM) compounds to meet specific application requirements [3–6]. Al containing compounds are known to increase the resistivity and ductility [3]. TbDyFeCo obtains optimum magnetostrictive properties over a wide temperature range [4]. High hardness and large magnetostriction at low field are achieved in Be-doped $Tb_{0.3}Dy_{0.7}Fe_{1.95}$ alloy [5]. Less than 15% B addition for Fe is used for increasing the room temperature magnetostriction [6].

At present, due to the very low electrode potential and high oxygen affinity of the rare-earth elements [7], electrochemical corrosion tend to occur to TbDyFe alloy even in humid atmosphere or seawater, which results in a severe drop or even total loss of the magnetostriction. This limits further application of TbDyFe alloy. But the corrosion resistance had been seldom investigated.

In this work, Si element is considered to be added into TbDyFe alloy aiming for developing giant magnetostrictive materials with improved corrosion resistance.

2. Experimental procedures

Starting materials with the nominal composition of $Tb_{0.3}Dy_{0.7}(Fe_{1-x}Si_x)_{1.95}$ ($x = 0$, 0.025 and 0.10) were prepared by arc melting the pure elements in a high-purity argon atmosphere, and then cast into rods with a diameter of 6 mm. The purities of the constituents are 99.98% for Tb, Dy, Fe, and 99.99% for Si. A Regaku D/max 2200 pc X-ray diffractometer with Cu Kα radiation was used to determine the structures. Specimens for corrosion resistance tests were cut by using a spark cutting, then polished to columns with the dimension of Ø 6 mm × 5 mm, all specimens were sealed with epoxy resin with one cross section surface outside. The only naked surface was carefully polished to avoid the possible measuring errors followed by cleaning in distilled water and alcohol before corrosion testing.

Samples with the composition of $Tb_{0.3}Dy_{0.7}(Fe_{1-x}Si_x)_{1.95}$ ($x = 0$, 0.025 and 0.10) in powder form were step scanned at a high Bragg angle 2θ ranging from 72.5° to 73.5° in order to calculate the spontaneous magnetostriction λ_{111}. The doubly split (4 4 0) XRD diffraction method was used to determine the spontaneous magnetostriction λ_{111} The magnetostriction was measured by the standard resistive str ain gauge method with sample dimension of Ø 6 mm × 25 mm. Electrochemical corrosion behaviors of the alloys were investigated by using potentiodynamic anodic polarization method on a HDV-7 electrochemical corrosion testing apparatus in 3.5 wt.% NaCl solution. The polarization scanning started at the steady open-circuit potential. The potentiodynamic anodic polarization curves in reference to a standard calomel electrode (SCE) were measured

* Corresponding author. Tel.: +86 10 82338780; fax: +86 10 82338200.
E-mail address: jiangcb@buaa.edu.cn (C. Jiang).

0925-8388/$ – see front matter © 2007 Elsevier B.V. All rights reserved.
doi:10.1016/j.jallcom.2007.01.072

at a scanning rate of 5 mV/s. The potential of the SCE is 0.244 V. Morphologies of the samples before and after the corrosion testing were observed with scanning electron microscope (SEM). Energy dispersive X-ray detector (EDX) was used to determine the compositions.

3. Results and discussion

Fig. 1(a) shows the X-ray diffraction patterns for powder samples of $Tb_{0.3}Dy_{0.7}(Fe_{1-x}Si_x)_{1.95}$ ($x=0$, 0.025 and 0.10). All the samples exhibit $MgCu_2$-type cubic Laves-phase structure. Si substitution for Fe does not change the structure. SEM backscattered morphology of $Tb_{0.3}Dy_{0.7}(Fe_{0.975}Si_{0.025})_{1.95}$ as-cast sample is shown in Fig. 1(b). An equiaxed biphase structure is observed with the gray rare-earth rich phase (R-rich phase) and the black Laves phase (matrix phase) because of the divorced eutectic reaction [8]. The tough rare earth-rich second phase distributes around the brittle matrix phase RFe_2 (or $R(Fe,Si)_2$), which is considered as an effective protection of the matrix phase [9]. Similar morphologies are found in $Tb_{0.3}Dy_{0.7}(Fe_{1-x}Si_x)_{1.95}$ ($x=0$ and 0.1) alloys. Fig. 1(c) shows the EDX results of as-cast $Tb_{0.3}Dy_{0.7}(Fe_{0.975}Si_{0.025})_{1.95}$ sample, from which we can see that Si content in rare earth-rich phase is higher than that in the matrix phase assigning in Fig. 1(b). $Tb_{0.3}Dy_{0.7}(Fe_{0.9}Si_{0.1})_{1.95}$ sample has the similar result.

For the Laves phase with easy magnetization direction (EMD) lying along the ⟨1 1 1⟩ axis [10], the spontaneous magnetostriction $\lambda_{1\,1\,1}$ can be obtained from the doubly split (4 4 0) XRD line in the inserted XRD diffraction pattern in Fig. 2(a), measured by the step-scanned method. The (4 4 0) reflection can be considered as a superposition of two separate diffracted $k\alpha_1$, $k\alpha_2$ profiles reflected from two separate lattices with a small difference in their interplaner distance [11]. After eliminating the peak of $k\alpha_2$, the value of $\lambda_{1\,1\,1}$ can be calculated from $\lambda_{1\,1\,1}=\Delta\alpha$ as plotted in Fig. 2(a), where $\Delta\alpha$ is the deviation of the angle between neighboring edges of the distorted cube from $\pi/2$ [12]. It can be seen that $\lambda_{1\,1\,1}$ decreases with increasing Si content in TbDyFeSi alloys, due to the negative contribution to the magnetostriction from the Si sublattice [13]. When $x=0$, $\lambda_{1\,1\,1}$ for traditional $Tb_{0.3}Dy_{0.7}Fe_{1.95}$ alloy is 1571 ppm, which is similar to the 1600 ppm of the previous studies about $Tb_{0.3}Dy_{0.7}Fe_2$ alloy [14,15]. For smaller Si content with $x=0.025$, $Tb_{0.3}Dy_{0.7}(Fe_{0.975}Si_{0.025})_{1.95}$ alloy shows a slightly decreased magnetostriction with the value of $\lambda_{1\,1\,1}$ around 1500 ppm. With further Si content for $x=0.1$, $\lambda_{1\,1\,1}$

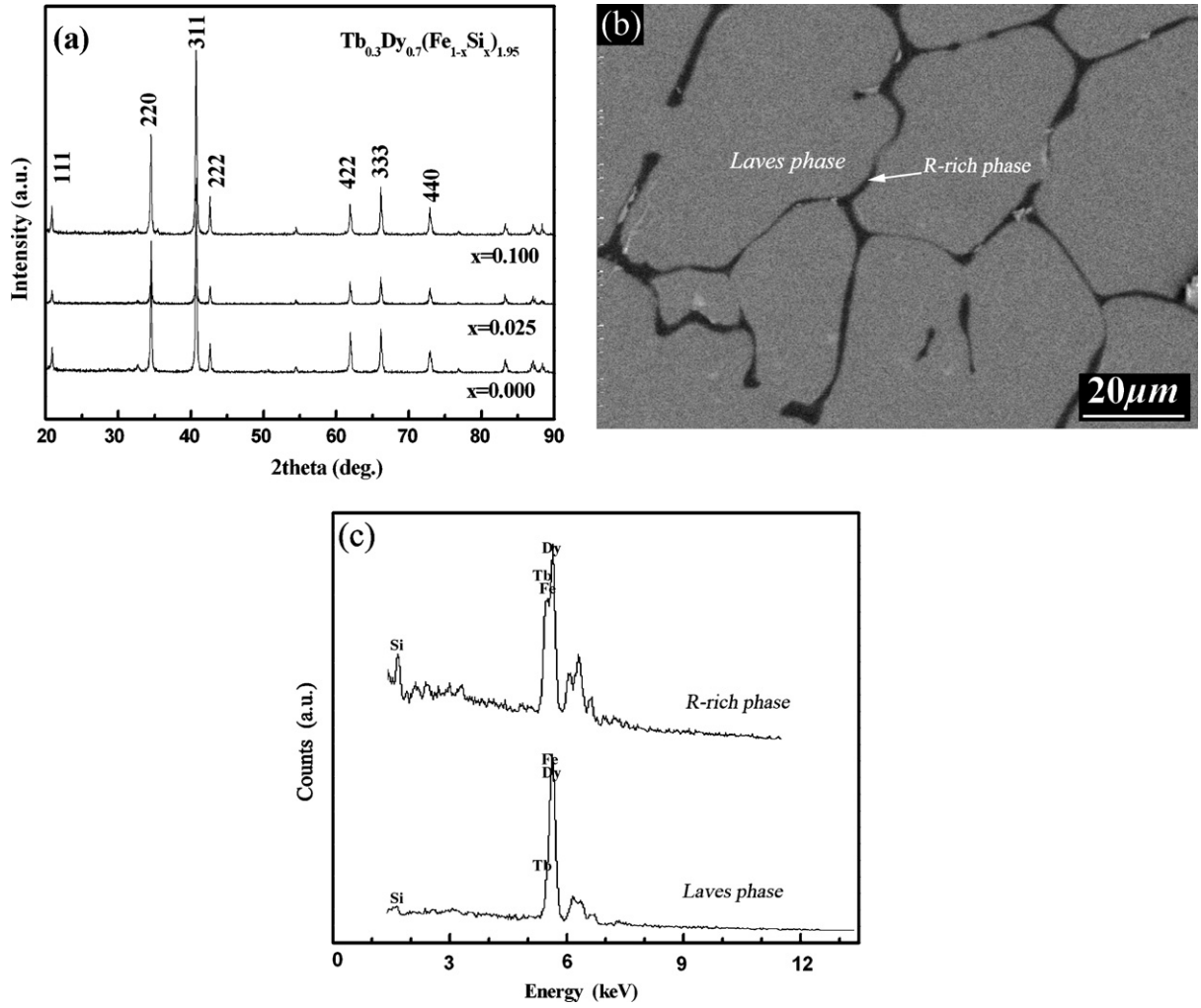

Fig. 1. Powder X-ray diffraction patterns (a), SEM backscattered morphology (b) and EDX results (c) of as-cast $Tb_{0.3}Dy_{0.7}(Fe_{0.975}Si_{0.025})_{1.95}$ alloy.

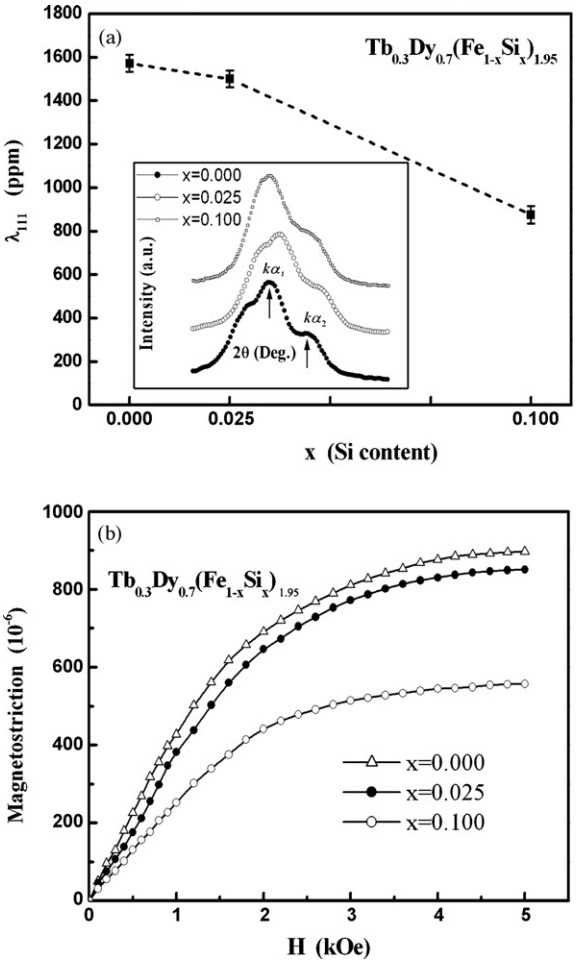

Fig. 2. Magnetostriction of as-cast TbDyFeSi alloys: (a) calculated spontaneous magnetostriction λ_{111} of $Tb_{0.3}Dy_{0.7}(Fe_{1-x}Si_x)_{1.95}$ ($x=0$, 0.025 and 0.1) and the insert is the profiles of the (4 4 0) line; (b) magnetostriction λ of as-cast $Tb_{0.3}Dy_{0.7}(Fe_{1-x}Si_x)_{1.95}$ ($x=0$, 0.025 and 0.1) samples at room temperature.

is drastically decreased to 875 ppm, which implies that further Si addition is obviously harmful to the magnetostrictive property. Fig. 2(b) shows the magnetostrictive properties of as-cast $Tb_{0.3}Dy_{0.7}(Fe_{1-x}Si_x)_{1.95}$ ($x=0$, 0.025 and 0.1) alloys at room temperature. The maximum magnetostriction in 5 kOe magnetic field under free conditions, which is near and taken as the saturated magnetostriction λ_s, decreases from 897×10^{-6} for $x=0$ to 851×10^{-6} for $x=0.025$ and 557×10^{-6} for $x=0.1$. Due to the saturated magnetostriction λ_s is approximately equal to $0.6\lambda_{111}$ for TbDyFe magnetostrictive alloy [1]; the tested values of λ_s are consistent with the calculated decreasing spontaneous magnetostriction λ_{111} for the TbDyFeSi alloys.

Fig. 3 shows the anodic polarization curves of TbDyFeSi alloys in 3.5 wt.% NaCl solution at room temperature. The natural corrosion potential E_{corr} and the anodic current density are introduced to evaluate the corrosion resistance. E_{corr} is the potential when there is no corrosion current flow in the external circuit, which indicates the thermodynamic susceptibility of the material to corrosion. E_{corr} is increased with Si addition in the TbDyFe alloys, with the values of −0.987, −0.959 and −0.915 V for $x=0$, 0.025 and 0.1, respectively, indicating the increased corrosion resistance. The anodic current density is proportional to the corrosion rate [16]. Thus, the corrosion rates could be compared by the anodic current densities at the same potential. From Fig. 3 we can see that with increasing Si addition, the polarization curve shifts to more positive, TbDyFeSi alloys possess lower anodic current densities than traditional TbDyFe alloy at a specific potential, indicating the decreasing corrosion rate.

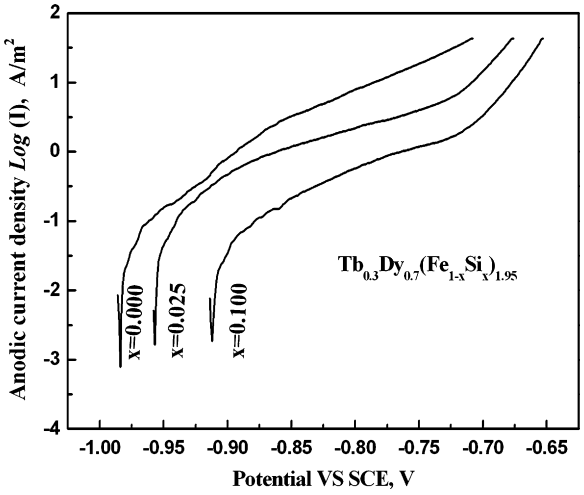

Fig. 3. Potentiodynamic anodic polarization curves of $Tb_{0.3}Dy_{0.7}(Fe_{1-x}Si_x)_{1.95}$ ($x=0$, 0.025 and 0.1) in 3.5 wt.% NaCl aqueous solution.

The results in Fig. 3 clearly demonstrate that TbDyFeSi alloys have better corrosion resistance than TbDyFe alloy in 3.5% NaCl solution, which is characterized by the higher E_{corr} and lower anodic current density. It is worth noting that the corrosion resistance could be increased obviously for little Si element content $Tb_{0.3}Dy_{0.7}(Fe_{0.975}Si_{0.025})_{1.95}$ alloy. Referring to the relative large magnetostriction λ_s as shown in Fig. 2 $Tb_{0.3}Dy_{0.7}(Fe_{0.975}Si_{0.025})_{1.95}$ alloy might be a good candidate possessing both giant magnetostriction and improved corrosion resistance. With further Si addition, the corrosion resistance of $Tb_{0.3}Dy_{0.7}(Fe_{0.9}Si_{0.1})_{1.95}$ is increased at the expense of the magnetostrictive property as indicated in Fig. 2.

After anodic polarization in 3.5% NaCl solution, the surface morphologies of the as-cast $Tb_{0.3}Dy_{0.7}Fe_{1.95}$ and $Tb_{0.3}Dy_{0.7}(Fe_{0.975}Si_{0.025})_{1.95}$ samples were studied by SEM, as shown in Fig. 4.

From Fig. 4(a) we can see that for $Tb_{0.3}Dy_{0.7}Fe_{1.95}$ alloy, the rare earth-rich phase is greatly corroded with extensive exfoliation of the matrix phase. Fig. 4(b) is the morphology of $Tb_{0.3}Dy_{0.7}$ $(Fe_{0.975}Si_{0.025})_{1.95}$ after corrosion test. Comparing with Fig. 4(a), the corrosion attack in Fig. 4(b) is obviously reduced with no apparent exfoliation of the matrix $R(Fe,Si)_2$ Laves phase, a relative smooth and compact surface is maintained.

Because of the electrochemically active characteristic, $Tb_{0.3}Dy_{0.7}Fe_{1.95}$ alloy tends to be corroded intensively in the forced corrosion test, leading to a high anodic current density in Fig. 3. On the other hand, as mentioned in Fig. 1(b), as-cast TbDyFe alloy and TbDyFeSi alloys consist of the net-shaped rare earth-rich phase and the equiaxed matrix phase. The rare earth-rich phase is electrochemically active with low E_{corr}

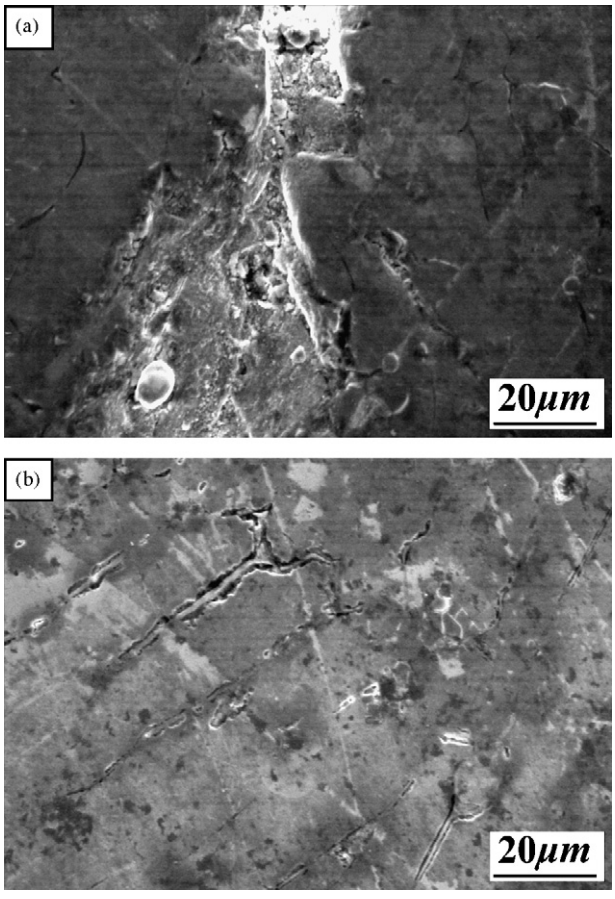

Fig. 4. SEM surface morphology after corrosion test of $Tb_{0.3}Dy_{0.7}$ $Fe_{1.95}$ alloy (a), and $Tb_{0.3}Dy_{0.7}(Fe_{0.975}Si_{0.025})_{1.95}$ alloy (b).

compared with that of the matrix phase. Under electrochemical condition, galvanic couple forms between the rare earth-rich phase and the matrix phase, and the rare earth-rich phase acts as anode against the matrix phase. Because of the low E_{corr}, rare earth-rich phase corrodes preferentially leading to intergranular corrosion. Furthermore, there exists a large difference in volume fraction between the matrix phase and the rare earth-rich phase, which means that a small amount of anodic phase connects to a large amount of cathodic phase. As a result, the rare earth-rich phase corrodes firstly with a high corrosion rate. With the extensive corrosion of the rare earth-rich phase, the matrix Laves phase breaks off by loosing the contact with the rare earth-rich phase, which is analogous to the exfoliation mechanism of the matrix phase in Nd–Fe–B alloy Gurrappa ever introduced [17].

Si addition is suggested to be responsible for the increase of the corrosion resistance in TbDyFeSi alloys. High Si-doped rare earth-rich phase is expected to possess an increased electrode potential, resulting in the raised E_{corr} value and improved corrosion-resistant of TbDyFeSi alloys. On other hand, the increased electrode potential reduces the electrochemical potential difference between the rare earth-rich phase and the matrix phase, leading to the lower anodic current density. Bala [18] offered similar explanation on the improved corrosion resistance for Cr-doped Nd–Fe–B alloy.

4. Conclusions

Improved corrosion resistance in 3.5 wt.% NaCl aqueous solution was achieved by using a small amount Si addition in $Tb_{0.3}Dy_{0.7}(Fe_{0.975}Si_{0.025})_{1.95}$ magnetostrictive alloy without obviously deteriorating the magnetostrictive property. The reason is suggested to be the increased E_{corr} for rare earth-rich phase and the reduction of the electrochemical potential difference between the rare earth-rich phase and the matrix phase of the alloys with Si addition.

Acknowledgements

This research was supported by the New Century Program for Excellent Talents of Ministry of Education of China (Grant No. NCET-04-0165) and the National Natural Science Foundation of China (Grant No. 60534020).

References

[1] A.E. Clark, in: E.P. Wohlfarth (Ed.), Ferromagnetic Materials I, North-Holland, Amsterdam, 1980, p. 531.
[2] X.G. Zhao, D.G. Lord, J. Magn. Magn. Mater. 195 (1999) 699.
[3] K. Prajapati, A.G. Jenner, M.P. Schulze, R.D. Greenough, J. Appl. Phys. 73 (1993) 6171.
[4] T.Y. Ma, C.B. Jiang, H.B. Xu, Appl. Phys. Lett. 86 (2005) 162505–162511.
[5] J.S. Shin, T.S. Chin, C.A. Chen, J. Magn. Magn. Mater. 191 (1999) 101.
[6] L. Wu, W.S. Zhan, X.C. Chen, J. Alloys Compd. 216 (1994) 85.
[7] B.D. Yan, G.W. Warren, M.H. Kim, J.A. Barnard, J. Appl. Phys. 67 (1990) 5310.
[8] O. Kubaschewski, Iron-Binary Phase Diagrams, Springer-Verlag, Berlin, 1982, pp. 108–111.
[9] P. Westwood, J.S. Abell, K.C. Pitman, J. Appl. Phys. 67 (1990) 4998.
[10] J.R. Cullen, A.E. Clark, Phys. Rev. B. 15 (1977) 4510.
[11] M. Al-Jiboory, D.G. Lord, IEEE. Trans. Magn. 26 (1990) 2583.
[12] R.Z. Levitin, A.S. Markosyan, J. Magn. Magn. Mater. 84 (1990) 247.
[13] L. Wu, W.S. Zhan, X.C. Chen, J. Alloys Compd. 255 (1997) 236.
[14] W.J. Ren, Z.D. Zhang, X.G. Zhao, W. Liu, D.Y. Geng, Appl. Phys. Lett. 84 (2004) 562.
[15] J.D. Verhoeven, E.D. Gibson, O.D. McMaster, H.H. Baker, Metall. Trans. A 18A (1987) 223.
[16] N. Eliaz, D.B. Mitton, N.J. Cantini, Mater. Technol. Adv. Perf. Mater. 16 (2000) 90.
[17] I. Gurrappa, J. Alloys Compd. 339 (2002) 241.
[18] H. Bala, G. Pawlowska, S. Szymura, V.V. Sergeev, Y.M. Rabinovich, J. Magn. Magn. Mater. 87 (1990) L255.